



Module 8

Spectral diagnostics for special environments – the interface between fusion and astrophysics

Lecture viewgraphs

Hugh Summers, Martin O'Mullane and Alessandra Giunta

University of Strathclyde

Contents

1. Introduction.
2. Emissivities, line ratio studies and contribution functions.
3. Differential emission measure (DEM) analysis.
4. Escape probabilities and opacity.
5. Non-Maxwellian electron distributions.

1.1 Atomic physics of astrophysical plasmas – the connection to fusion

Atomic physics of plasmas has application in many areas of astrophysics:

1. The solar upper atmosphere
2. Gaseous and diffuse nebulae
3. Emission from cometary plasma
4. Black hole accretion disks and columns

These areas emphasise particular plasma atomic physics scenarios, such as

- a. Electron-excited or photo-excited
- b. Tenuous or dense
- c. Optically thick or thin
- d. Transient or stationary
- e. Thermal or non-thermal electrons

We wish to explore if the ADAS studies of astrophysical plasmas can assist in analysing new situations of concern for current fusion plasma and ITER. It is evident that the **solar plasma** has exceptional spectral observations from spacecraft such as SOHO and can give us special insight.

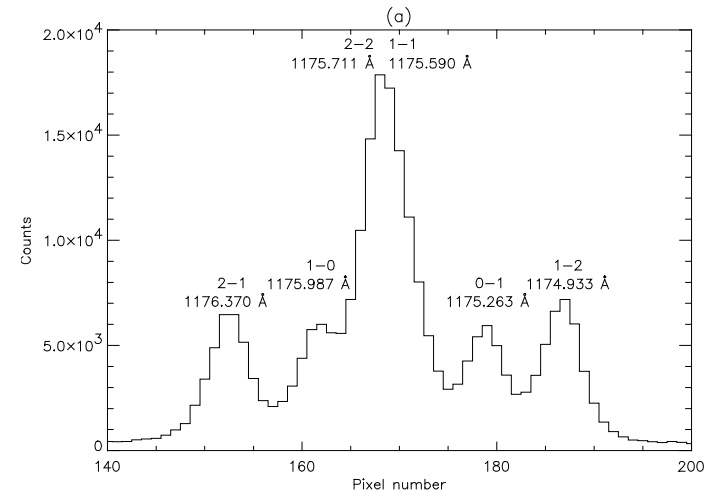
This means atomic physics parameter space of: a - **electron excited**; b - **low to intermediate density**; c - **mostly thin**; d - **both**; e – **mostly thermal**.

1.2 SUMER spectrum lines from CIII

The top figure shows a small portion of a spectrum is from the SUMER UV spectrometer on the SOHO spacecraft looking at the sun.

It shows J-resolved components of the CIII ($2s2p\ ^3P - 2p^2\ ^3P$) multiplet.

CIII lines are important in deducing lower chromosphere density/variation with height, that is **emission measure**.

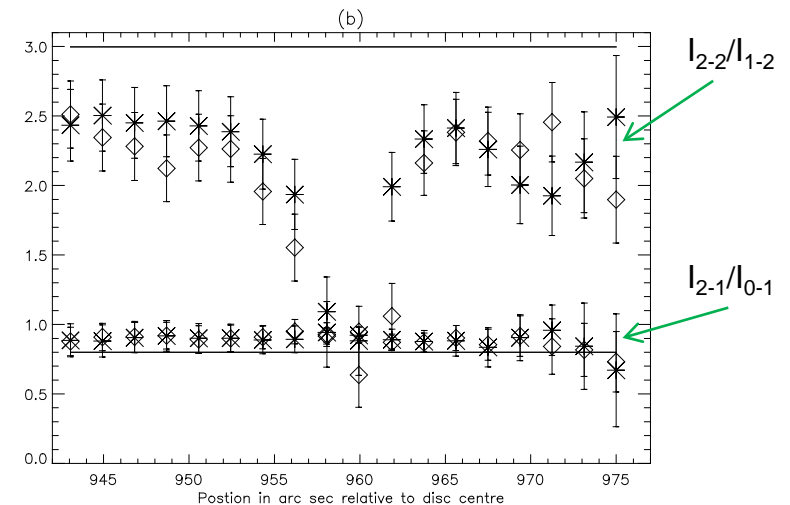


The lower figure shows two ratios of different component line intensities - the upper is 2-2/1-2 and the lower 0-1/2-1.

Observations are made at different positions scanning across the limb of the sun.

Both the lines of each ratio originate from the same upper level.

These are **electron-excited** lines and one ratio shows the effects of **opacity** at the limb.



1.3 Approximate photon emissivities

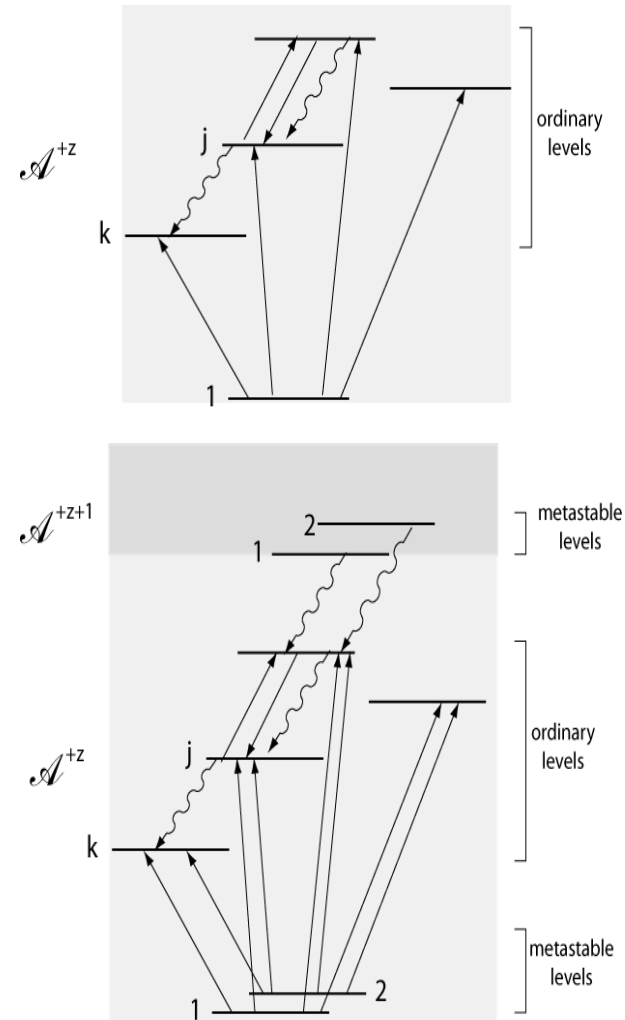
Excited population modelling solves the statistical balance equations of an ion \mathcal{A}^{+Z} . Most simply, the excited populations N_j are solved in equilibrium with respect to the ground population N_1 . Then the emissivity in a transition j to k is

$$\epsilon_{j \rightarrow k} = A_{j \rightarrow k} N_j = \mathcal{P} \mathcal{E} \mathcal{C}_{j \rightarrow k} N_e N_1$$

Properly

$$\epsilon_{j \rightarrow k} = A_{j \rightarrow k} \left(\sum_{\sigma=1}^{M^{(z)}} \mathcal{F}_{j\sigma}^{(exc)} N_e N_{\sigma} + \sum_{\nu'=1}^{M^{(z+1)}} \mathcal{F}_{j\nu'}^{(rec)} N_e N_{\nu'}^+ + \sum_{\nu'=1}^{M^{(z+1)}} \mathcal{F}_{j\nu'}^{(CX)} N_H N_{\nu'}^+ + \sum_{\mu'=1}^{M^{(z-1)}} \mathcal{F}_{j\mu'}^{(ion)} N_e N_{\mu'}^- \right)$$

where excited, N_j , and metastable, N_{σ} , populations are distinguished, and solution is for excited populations in quasi-equilibrium with metastables. Recombination, charge exchange and inner shell ionisation are included – called generalised-collisional-radiative, **GCR**, modelling.



1.4 Generalised collisional-radiative photon emissivities

The partial photon emissivity coefficients are prepared and archived as ADAS data format ADF15.

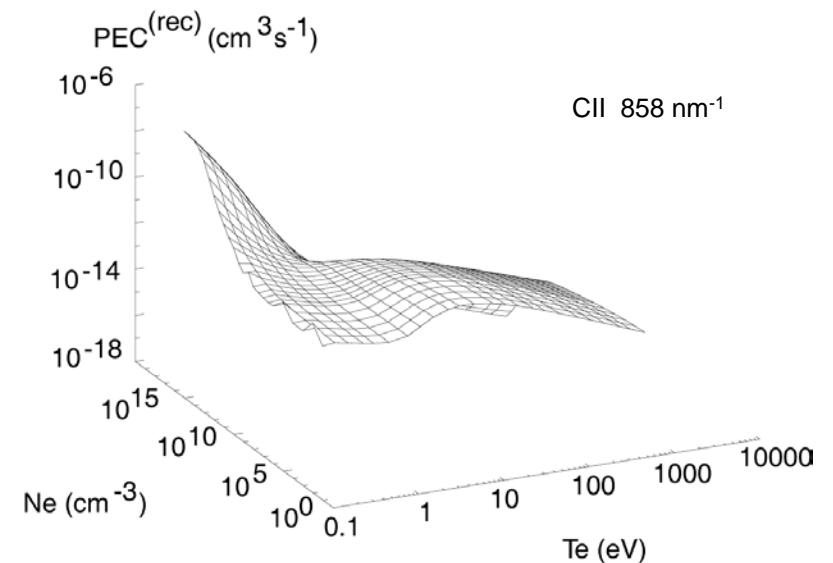
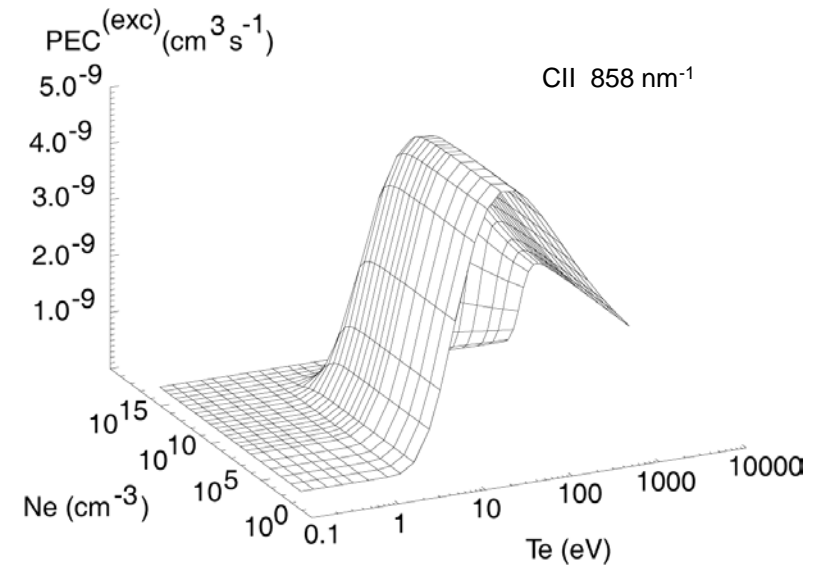
$$\mathcal{P}\mathcal{E}\mathcal{C}_{\sigma,j\rightarrow k}^{(exc)} = A_{j\rightarrow k}\mathcal{F}_{j\sigma}^{(exc)}$$

$$\mathcal{P}\mathcal{E}\mathcal{C}_{\nu',j\rightarrow k}^{(rec)} = A_{j\rightarrow k}\mathcal{F}_{j\nu'}^{(rec)}$$

$$\mathcal{P}\mathcal{E}\mathcal{C}_{\nu',j\rightarrow k}^{(CX)} = A_{j\rightarrow k}\mathcal{F}_{j\nu'}^{(CX)}$$

$$\mathcal{P}\mathcal{E}\mathcal{C}_{\sigma,j\rightarrow k}^{(ion)} = A_{j\rightarrow k}\mathcal{F}_{j\mu'}^{(ion)}$$

They are resolved by transition, primary driver, metastable and depend on T_e and N_e in general.



2.1 Emissivities and line ratio studies.

For two lines driven primarily by excitation, the intensity ratio is can be simpler for diagnostic deductions. It is usually helpful to work with line sets. If recombination is ignored

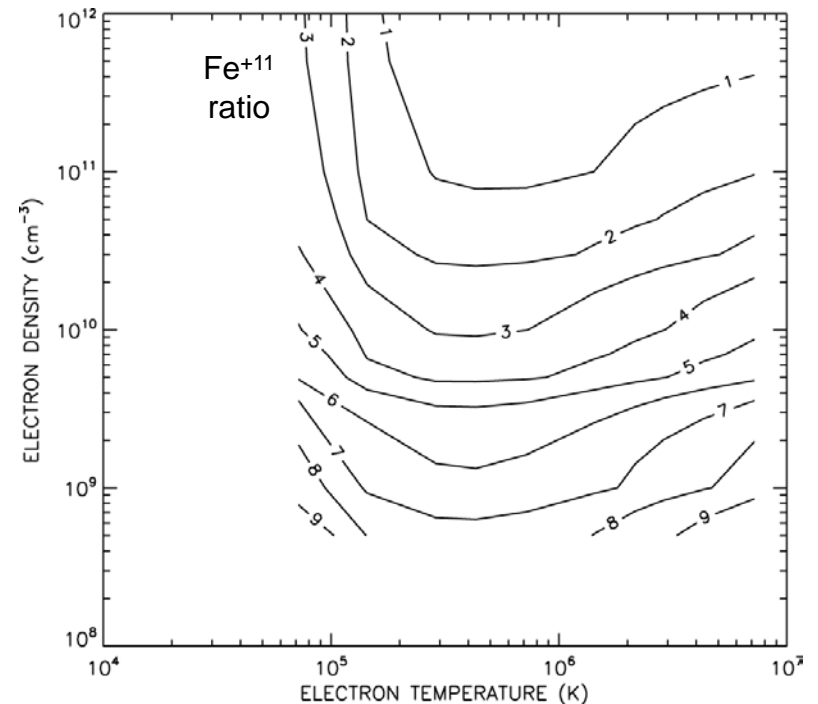
$$\frac{\epsilon_{G_1}}{\epsilon_{G_2}} = \frac{\sum_{j \in J_G, k \in K_G} \mathcal{P} \mathcal{E} \mathcal{C}_{1, j \rightarrow k}^{(exc)} + N_e N_1 \sum_{j \in J_G, k \in K_G} \sum_{\sigma, \sigma \neq 1} \mathcal{P} \mathcal{E} \mathcal{C}_{\sigma, j \rightarrow k}^{(exc)} \left(\frac{N_\sigma}{N_1} \right)}{\sum_{j' \in J'_G, k' \in K'_G} \mathcal{P} \mathcal{E} \mathcal{C}_{1, j' \rightarrow k'}^{(exc)} + N_e N_1 \sum_{j' \in J'_G, k' \in K'_G} \sum_{\sigma', \sigma' \neq 1} \mathcal{P} \mathcal{E} \mathcal{C}_{\sigma', j' \rightarrow k'}^{(exc)} \left(\frac{N_{\sigma'}}{N_1} \right)}$$

Then, the character of the metastables must be considered. If

$$\left(\frac{N_\sigma}{N_1} \right) \approx \left(\frac{N_\sigma}{N_1} \right)_{eq} \quad \text{or} \quad \approx 0$$

a ratio depending only on T_e and N_e results. Contour plots of the ratio show the important sensitivities. See [ADAS205](#), [ADAS207](#).

More careful approaches uses the PECs directly. See [run_adas208.pro](#), [read_adf15.pro](#).



2.2 Line-of-sight intensity

The intensity of emission in the spectrum line j to k from a column of plasma of area A .

$$I_{j \rightarrow k} = \frac{1}{4\pi A} \int \varepsilon_{j \rightarrow k} dV \quad [\text{photons cm}^{-2} \text{s}^{-1} \text{sr}^{-1}]$$

Consider the ionisation stages, \mathcal{A}^{+z} of element \mathcal{A} of nuclear charge z_0 . With $N_\sigma \equiv N_\sigma^{(z)}$

$$N_{tot} = \sum_{z=0}^{z_0} N^{(z)} = \sum_{z=0}^{z_0} \sum_{\sigma=1}^{M^{(z)}} N_\sigma^{(z)} \quad N_\sigma^{(z)} = \frac{N_\sigma^{(z)}}{N^{(z)}} \frac{N^{(z)}}{N_{tot}} \frac{N_{tot}}{N_H} \frac{N_H}{N_e} N_e$$

Then neglecting recombination contributions to emissivity

$$\begin{aligned} I_{j \rightarrow k} &= \frac{1}{4\pi A} \int_V \left(A_{j \rightarrow k} \sum_{\sigma=1}^{M^{(z)}} \mathcal{F}_{j\sigma}^{(exc)} \frac{N_\sigma^{(z)}}{N^{(z)}} \frac{N^{(z)}}{N_{tot}} \right) \frac{N_{tot}}{N_H} \frac{N_H}{N_e} N_e^2 dV \\ &\approx \frac{1}{4\pi A} \left(\frac{N_{tot}}{N_H} \right) \left(\frac{N_H}{N_e} \right) \int_V \left(A_{j \rightarrow k} \sum_{\sigma=1}^{M^{(z)}} \mathcal{F}_{j\sigma}^{(exc)} \frac{N_\sigma^{(z)}}{N^{(z)}} \frac{N^{(z)}}{N_{tot}} \right)_{eq} N_e^2 dV \end{aligned}$$

2.3 Contribution functions

The excitation contribution function or GTN-function for a general plasma is

$$\mathcal{G} \mathcal{J} \mathcal{N}_{j \rightarrow k}^{(exc)}(T_e, N_e) = \left(A_{j \rightarrow k} \sum_{\sigma=1}^{M^{(z)}} \mathcal{F}_{j\sigma}^{(exc)} \frac{N_{\sigma}^{(z)}}{N^{(z)}} \frac{N^{(z)}}{N_{tot}} \right)_{eq}$$

2-parm. family

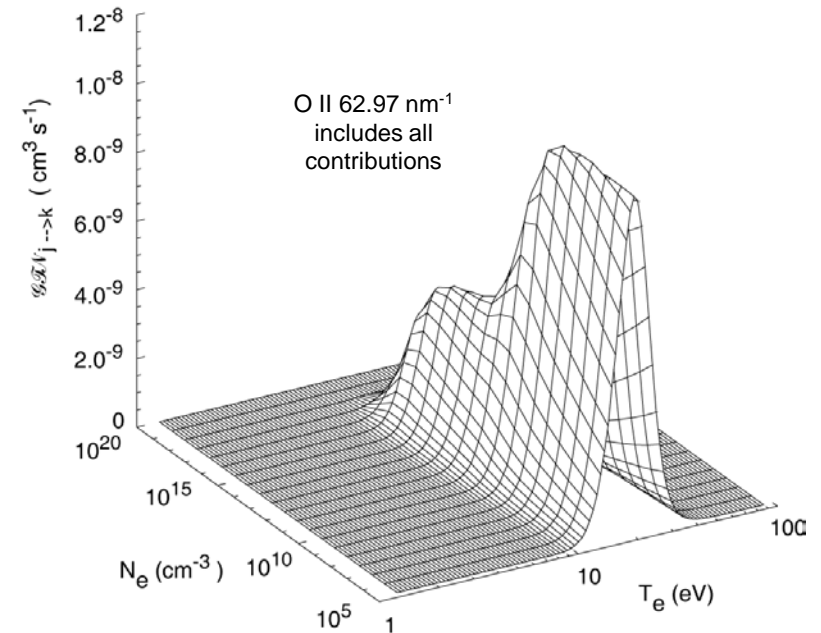
The solar astrophysical contribution function or GTe-function is

$$G_{j \rightarrow k}(T_e, N_e(T_e)) = \left(A_{j \rightarrow k} \sum_{\sigma=1}^{M^{(z)}} \mathcal{F}_{j\sigma}^{(exc)} \frac{N_{\sigma}^{(z)}}{N^{(z)}} \frac{N^{(z)}}{N_{tot}} \right)_{eq} \left(\frac{N_H}{N_e} \right)$$

1-parm. family

ADAS has facilities for preparing GTe-functions in format [adf20](#). See [ADAS412](#). It can select GTe-functions from adf20 into a collection file ready for DEM analysis. See [ADAS506](#).

ADAS can prepare GTN-functions of format [adf16](#) at the same time as executing an ionisation balance. See [ADAS405](#).



3.1 Differential emission measure (DEM) analysis.

Since $\frac{1}{A} \int N_e^2 dV \approx \int N_e^2 \frac{dh}{dT_e} dT_e$ define the differential emission measure as $\Phi(T_e) = N_e^2 \frac{dh}{dT_e}$

If $\mathcal{A}(z_0) = \frac{N_{tot}}{N_H}$ is the fractional abundance of the element of nuclear charge z_0 , then for a suitable

set of observed spectral intensities $I_i : i = 0, \dots, m$ with known theoretical GTE-functions

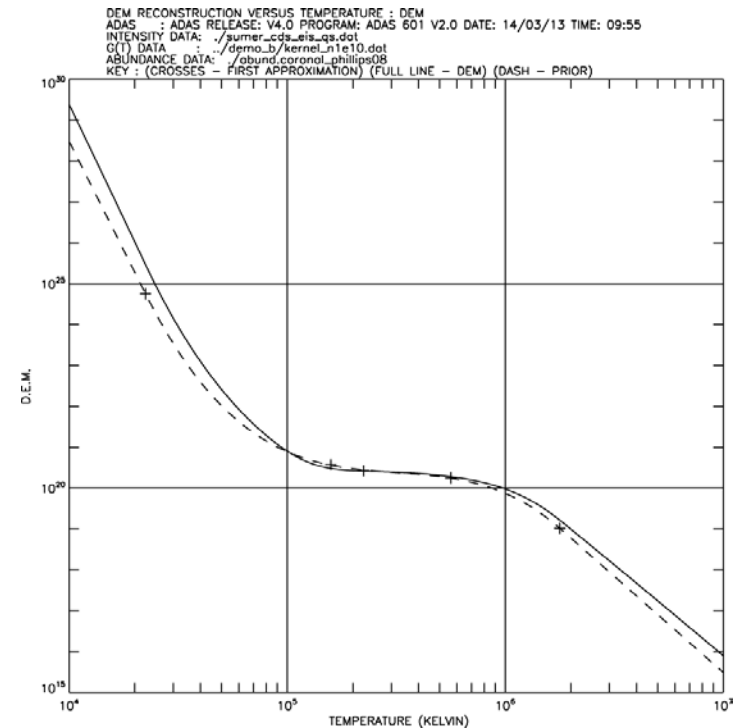
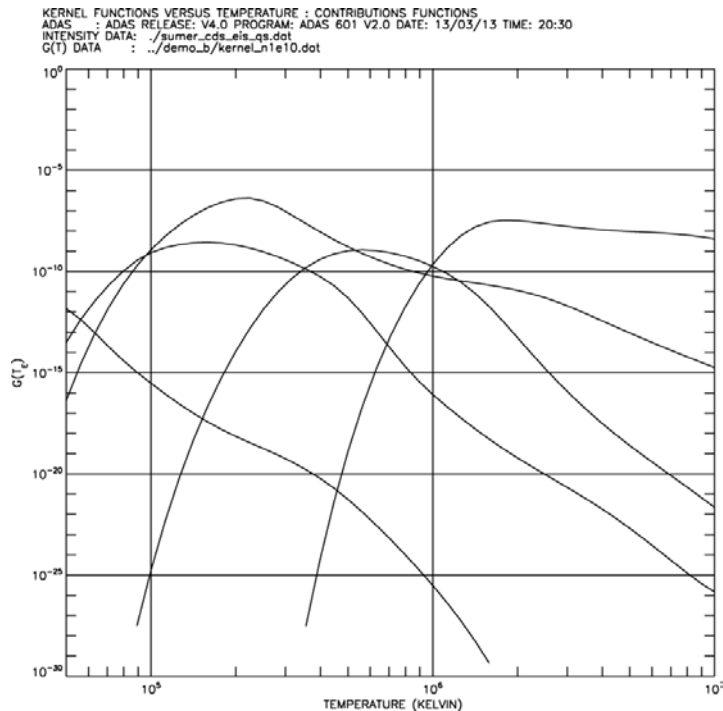
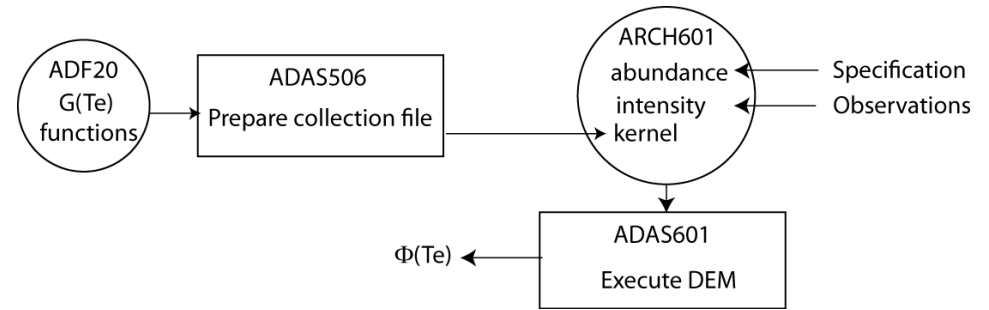
The integral equation $I_i = \frac{1}{4\pi} \int_{T_1}^{T_2} \mathcal{A}(z_0) G_i(T_e) \Phi(T_e) dT_e$ can be solved for the differential emission measure.

There is an extensive history of study and implementation of solutions of this system. ADAS uses the methodology of Thompson. ADAS staff and collaborators (Giunta & Lanzafame) have worked intensively on refinement of the method, implemented as code [ADAS601](#) - summarised in the notes for the lecture.

3.2 DEM implementation.

The schematic shows the principal ADAS steps, datasets and codes.

1. Collection of a targetted set of $G(T_e)$ functions spanning the required T_e range – shown below.
2. The final DEM – shown below right



4.1 Escape probabilities and opacity.

The emission from an optically thick plasma is characterised by the equations of radiative transfer and of statistical balance.

$$\frac{dI_\nu(s)}{ds} = j_\nu(s) - \kappa_\nu(s)I_\nu(s)$$

$$\frac{dN_u(\vec{r})}{dt} = -A_{u \rightarrow l}N_u(\vec{r}) + \frac{4\pi}{c}B_{l \rightarrow u}N_l(\vec{r}) \int \bar{I}_\nu(\vec{r})\phi_a(\nu)d\nu$$

$$j_\nu(\vec{r}) = \frac{1}{4\pi}A_{u \rightarrow l}N_u(\vec{r})\phi_e(\nu)$$

$$\kappa_\nu(\vec{r}) = \frac{1}{c}N_l h\nu B_{l \rightarrow u}\phi_a(\nu)$$

↗
↖

emission coefficient
absorption coefficient

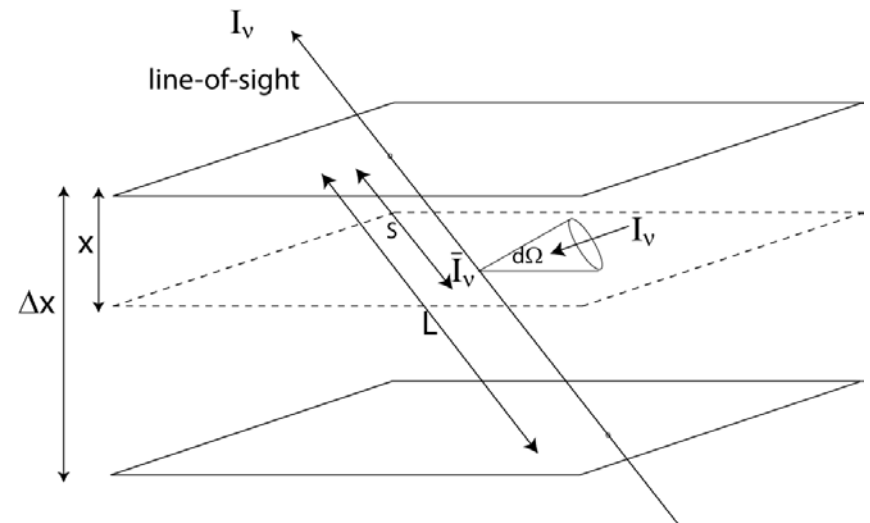
The equations can be rewritten as

$$\frac{dI_\nu(s)}{ds} = \frac{1}{4\pi}A_{u \rightarrow l}N_u(s)g(s)$$

$$\frac{dN_u(\vec{r})}{dt} = -A_{u \rightarrow l}N_u(\vec{r})\Lambda(\vec{r}) + \text{other terms}$$

$g(s)$ is the **emergent flux escape factor**.

$\Lambda(\vec{r})$ is the **absorption factor** or **population escape factor**.



4.2 Line-of-sight averaged escape probability, $\bar{g}\{\tau_0\}$.

For Doppler emission and absorption profiles of Doppler width $\Delta\nu_D$

$$\phi_e(\nu) = \phi_a(\nu) \equiv \phi(\nu) = \frac{1}{\sqrt{\pi}\Delta\nu_D} \exp\left\{-\left(\frac{\nu - \nu_0}{\Delta\nu_D}\right)^2\right\}$$

With a line-of-sight $s : 0 \rightarrow L$

$$g(s) = \frac{1}{\sqrt{\pi}} \int_{-\infty}^{\infty} e^{-u^2} \exp\{-\tau_0(s)e^{-u^2}\} du$$

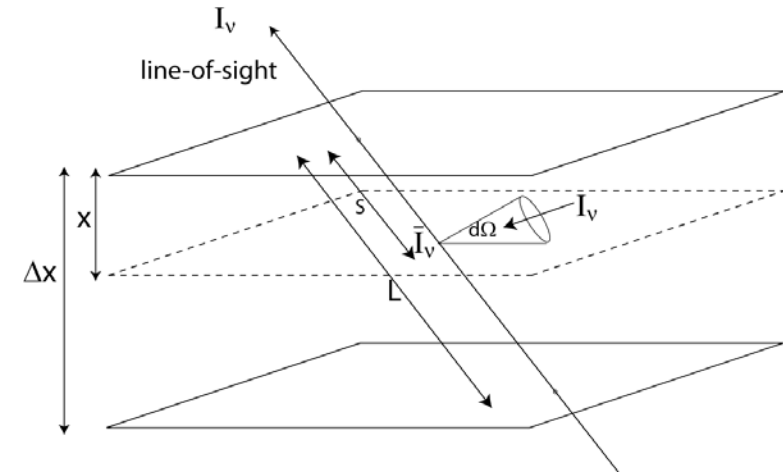
where $\tau_0(s) = \kappa_{0,l \rightarrow u}(L - s)$ is the line centre optical depth.

The total intensity, integrating through the layer, assuming constant density, is

$$I = \frac{1}{4\pi} A_{u \rightarrow l} N_u \bar{g}\{\tau_0\} L \quad \text{with} \quad \bar{g}\{\tau_0\} = \frac{1}{\sqrt{\pi}} \int_{-\infty}^{\infty} \left[\frac{1 - \exp\{-\tau_0 e^{-u^2}\}}{\tau_0} \right] du$$

and $\tau_0 \equiv \tau_0(s = 0) = 1.16^{-6} \sqrt{M/T_i} \lambda_0 N_l f_{l \rightarrow u} L$

[T_i in K, M in amu, lengths in cm]



4.3 The absorption factor, $\Lambda(\vec{r})$

$$\begin{aligned}
 \bar{I}_\nu &= \frac{1}{4\pi} \int_0^{4\pi} I_\nu(\theta, \phi) d\Omega \\
 &= \frac{1}{4\pi} \int_0^{4\pi} \frac{\kappa_\nu}{j_\nu} \left[1 - e^{-\tau_\nu(\theta, \phi)} \right] d\Omega \\
 &= \frac{\kappa_\nu}{j_\nu} \overline{\left[1 - e^{-\tau_\nu(\theta, \phi)} \right]} \\
 &= \frac{\kappa_\nu}{j_\nu} \left[1 - e^{-\overline{\tau_\nu(\theta, \phi)}} \right] \quad \text{where} \quad \overline{\tau_\nu(\theta, \phi)} = \kappa_0 \phi(\nu) \bar{L} = \bar{\tau}_0 \phi(\nu)
 \end{aligned}$$

Then

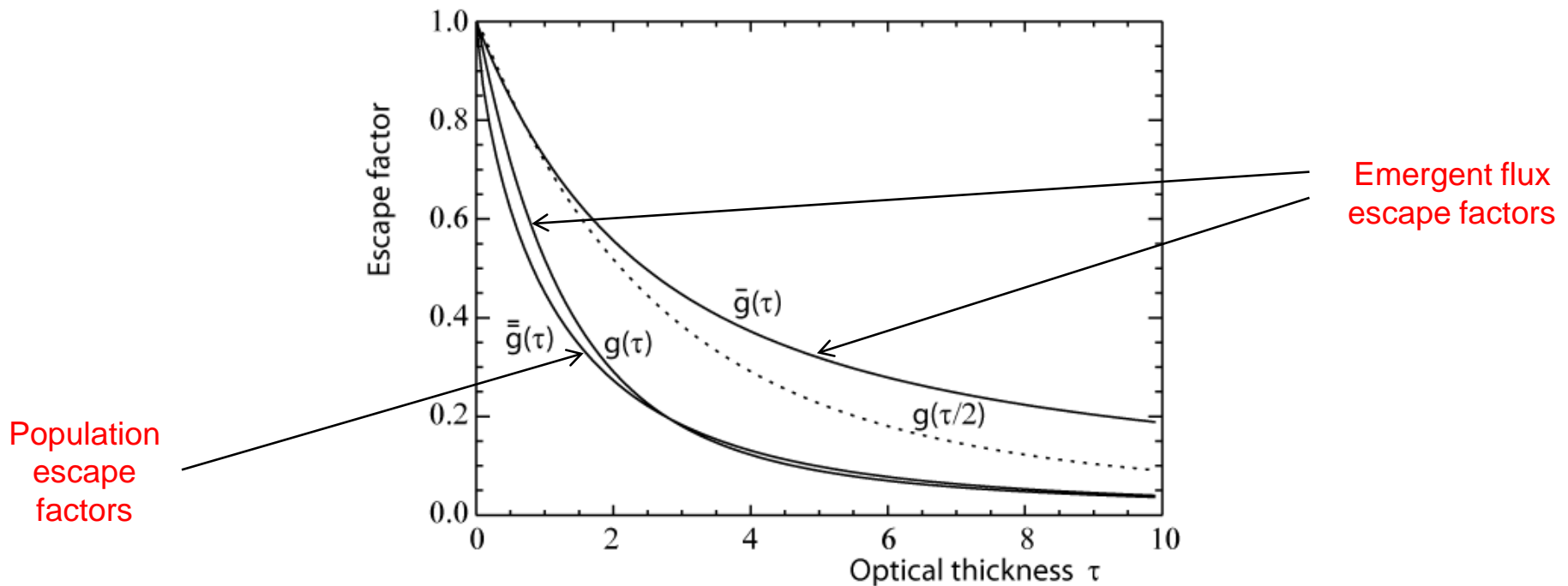
$$\Lambda(\vec{r}) = 1 - \frac{N_l(\vec{r}) \omega_u}{N_u(\vec{r}) \omega_l} \frac{c^2}{2\nu_0^2} \int \bar{I}_\nu(\vec{r}) \phi_a(\nu) d\nu$$

$$\Lambda(\vec{r}) = 1 - \frac{1}{\sqrt{\pi}} \int_{-\infty}^{\infty} \left[1 - \exp\{-\bar{\tau}_0 e^{-u^2}\} e^{-u^2} \right] du \equiv g\{\bar{\tau}_0\}$$

4.4 Various escape factors

For a semi-infinite layer of thickness D and perpendicular optical thickness τ_0 , at layer centre

$$\Lambda(\vec{r}) = \frac{1}{\sqrt{\pi}} \int_{-\infty}^{\infty} e^{-u^2} \left[\exp\left\{\frac{-\tau_0 e^{-u^2}}{2}\right\} - \left\{\frac{\tau_0 e^{-u^2}}{2}\right\} E_1\left\{\frac{\tau_0 e^{-u^2}}{2}\right\} \right] du \equiv \bar{g}\{\tau_0/2\}$$



4.5 Application to solar observations

For two lines with common upper level u and lower levels l_1 and l_2 , the observed intensity ratio is

$$\frac{\bar{I}_{u \rightarrow l_1}}{\bar{I}_{u \rightarrow l_2}} = \frac{A_{u \rightarrow l_1} \bar{g}\{\tau_{0, l_1 \rightarrow u}\}}{A_{u \rightarrow l_2} \bar{g}\{\tau_{0, l_2 \rightarrow u}\}}$$

but

$$\tau_{0, l_1 \rightarrow u} = \tau_{0, l_2 \rightarrow u} \frac{N_{l_1} f_{l_1 \rightarrow u}}{N_{l_2} f_{l_2 \rightarrow u}}$$

then find the $\tau_{0, l_1 \rightarrow u}$ which satisfies the intensity ratio taking the $\bar{g}(\tau)$ value ratio from the previous figure.

Infer the emergent flux escape factors and population escape factors for all other transitions from the ground or metastables.

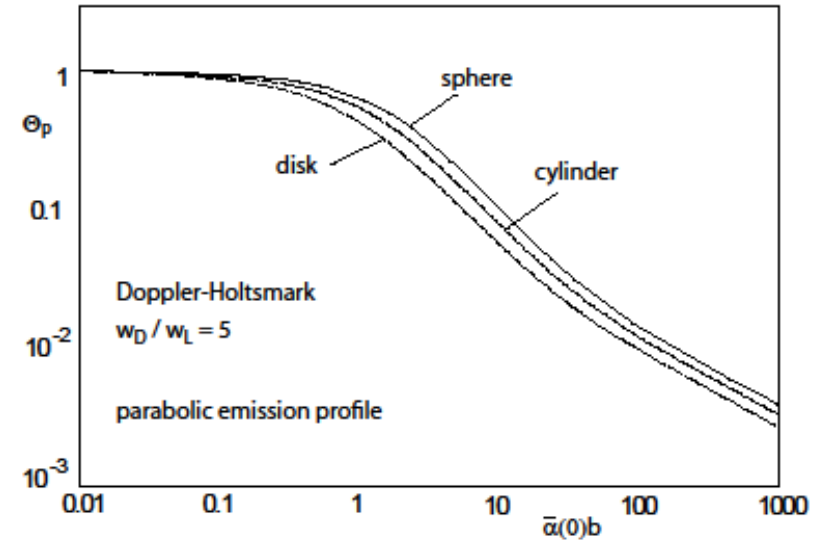
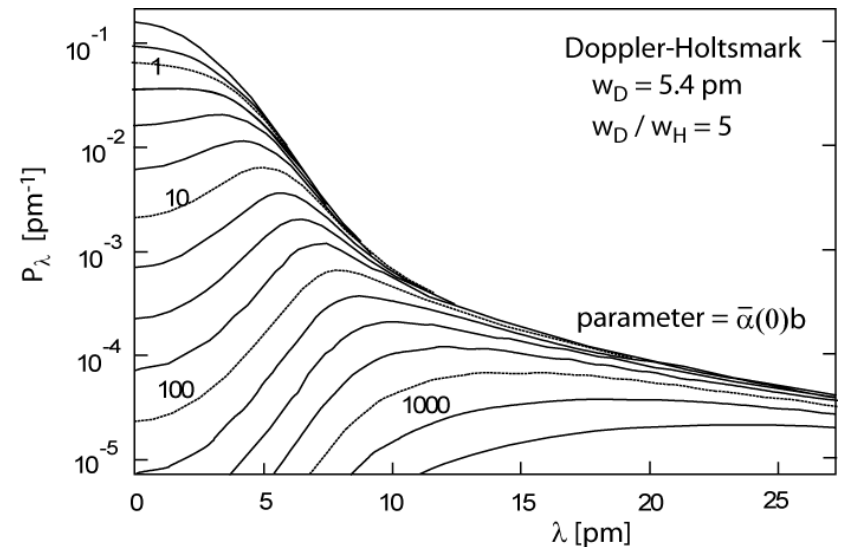
4.6 ADAS predictive modelling

ADAS214 calculates escape factors for emergent flux and for population calculations for simple plasma models and spectral line profiles.

Spectral profiles include Doppler, Lorentz, Holtsmark and convolutions of pairs of these.

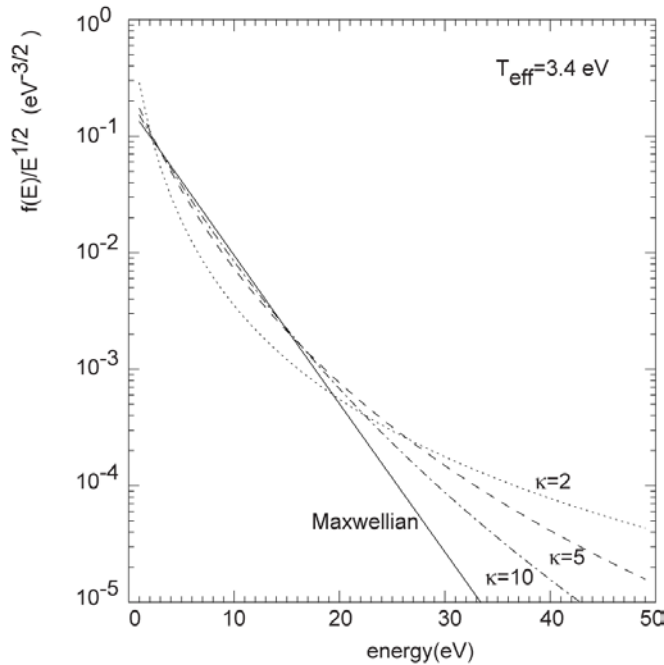
The population escape factor can be calculated in the centre of a plasma sphere, in the mid-plane of a disk and on the axis of a cylinder.

The code can be run for constant emission, linear or parabolic decrease from the plasma centre (or axis).

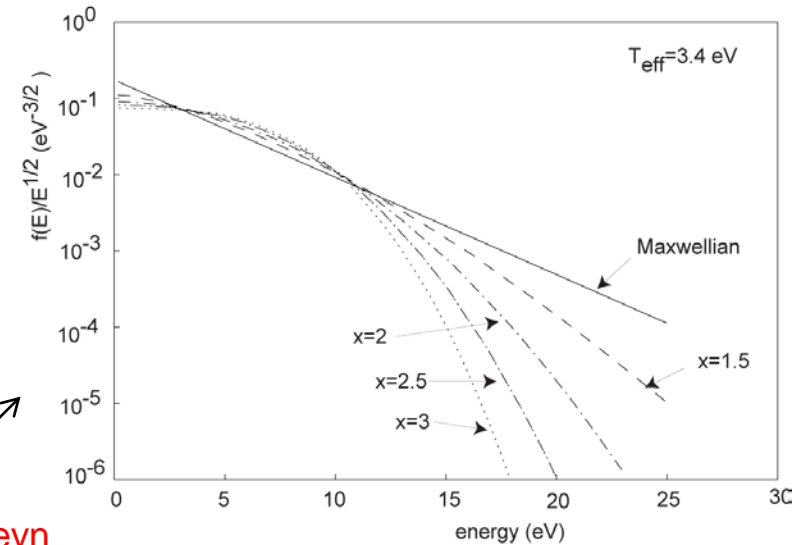


5.1 Non-Maxwellian electron distributions.

$$f_{T_e}(E) = \frac{1}{kT_e} \frac{2}{\sqrt{\pi}} \left(\frac{E}{kT_e} \right)^{1/2} \exp\left(-\frac{E}{kT_e}\right) \leftarrow \text{Maxwellian}$$



Kappa



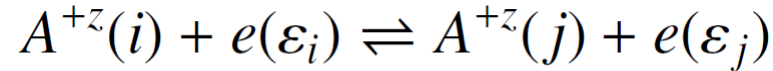
Druyvesteyn

$$f_{\kappa, E_{\kappa}}(E) = \frac{1}{E_{\kappa}} \frac{2}{\sqrt{\pi}} \left(\frac{E}{E_{\kappa}} \right)^{1/2} \kappa^{-3/2} \frac{\Gamma(\kappa + 1)}{\Gamma(\kappa - \frac{1}{2})} \left(1 + \frac{E}{\kappa E_{\kappa}} \right)^{-(\kappa+1)}$$

$$f_{x, E_x}(E) = \frac{x}{E_x^{3/2}} \frac{\Gamma(5/2x)^{3/2}}{\Gamma(3/2x)^{5/2}} E^{1/2} \exp\left(-\left[\frac{E\Gamma(5/2x)}{E_x\Gamma(3/2x)}\right]^x\right)$$

5.2 Reaction cross-sections and rate coefficients.

Consider the reaction



Maxwellian: detailed balance

$$\Upsilon_{ij}(T_e) = \int_0^\infty \Omega_{ij}(\varepsilon_j) \exp\left(-\frac{\varepsilon_j}{kT_e}\right) d\left(\frac{\varepsilon_j}{kT_e}\right)$$

$$q_{i \rightarrow j}(T_e) = 2\sqrt{\pi}\alpha c a_0^2 \left(\frac{I_H}{kT_e}\right)^{1/2} \frac{1}{\omega_i} \exp\left(-\frac{\Delta E_{ij}}{kT_e}\right) \Upsilon_{ij}(T_e)$$

$$q_{j \rightarrow i}(T_e) = 2\sqrt{\pi}\alpha c a_0^2 \left(\frac{I_H}{kT_e}\right)^{1/2} \frac{1}{\omega_j} \Upsilon_{ij}(T_e)$$

same

Non-Maxwellian: no detailed balance

$$\Upsilon_{i \rightarrow j}(T_{eff}) = \frac{\sqrt{\pi}}{2} \exp\left(\frac{\Delta E_{ij}}{kT_{eff}}\right) \int_0^\infty \Omega_{ij}(\varepsilon_i) \left(\frac{\varepsilon_i}{kT_{eff}}\right)^{-1/2} f(\varepsilon_i) d\varepsilon_j$$

$$\mathfrak{J}_{j \rightarrow i}(T_{eff}) = \frac{\sqrt{\pi}}{2} \int_0^\infty \Omega_{ij}(\varepsilon_j) \left(\frac{\varepsilon_j}{kT_{eff}}\right)^{-1/2} f(\varepsilon_j) d\varepsilon_j$$

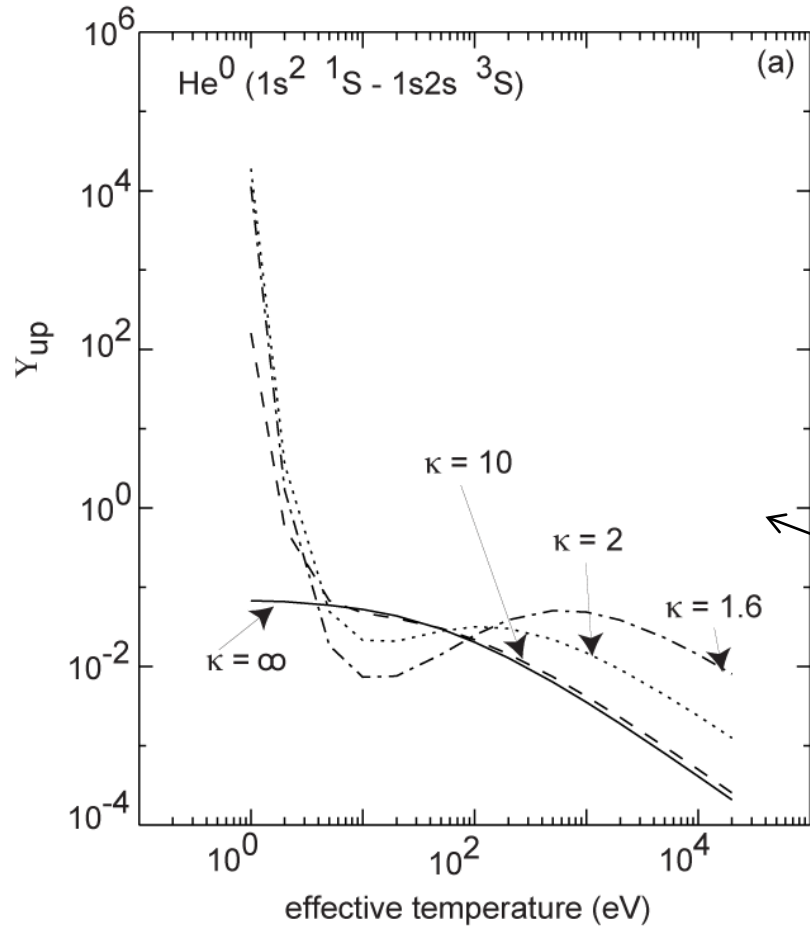
$$q_{i \rightarrow j}(T_{eff}) = 2\sqrt{\pi}\alpha c a_0^2 \left(\frac{I_H}{kT_{eff}}\right)^{1/2} \frac{1}{\omega_i} \exp\left(-\frac{\Delta E_{ij}}{kT_{eff}}\right) \Upsilon_{i \rightarrow j}(T_{eff})$$

$$q_{j \rightarrow i}(T_{eff}) = 2\sqrt{\pi}\alpha c a_0^2 \left(\frac{I_H}{kT_{eff}}\right)^{1/2} \frac{1}{\omega_j} \mathfrak{J}_{j \rightarrow i}(T_{eff})$$

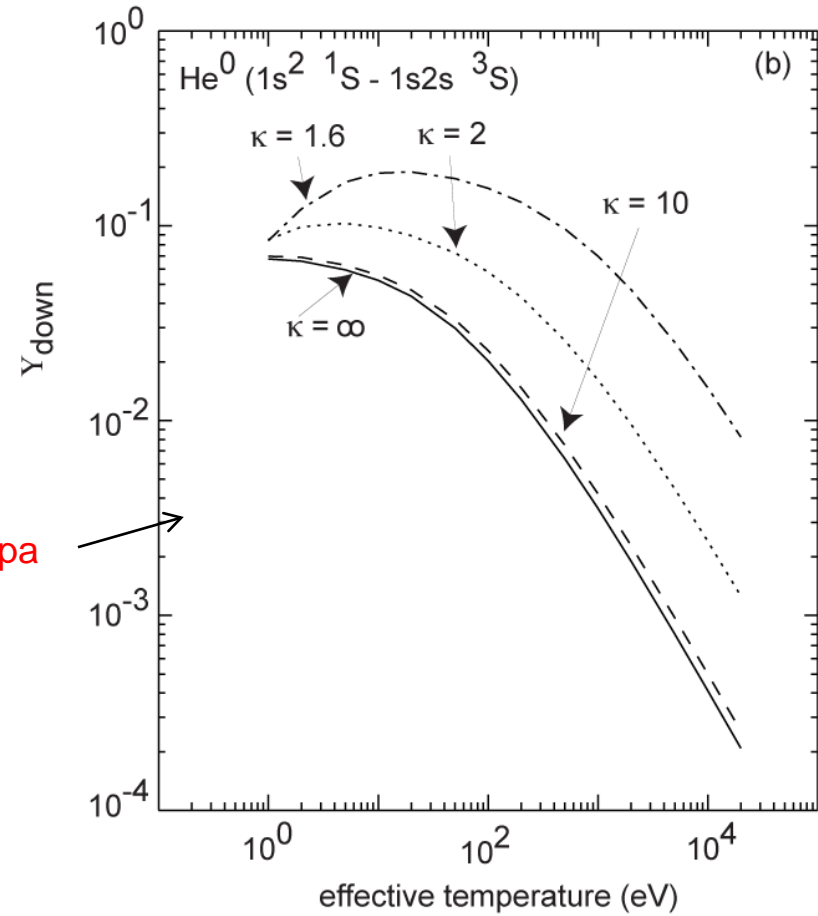
different

Effective mean energy parameter

5.3 Upsilon and downsilon



Kappa



5.4 Other rate coefficients

Dielectronic recombination and radiative recombination coefficients are straightforward. Electron impact ionisation and three-body recombination are more complicated.

Fowler relation is the starting point

$$\omega_i E Q_{i \rightarrow +}(E; E', E'') = \frac{16\pi m}{h^3} \omega_+ E' E'' Q_{+ \rightarrow i}(E', E''; E)$$

Collisional ionisation

$$q_{i \rightarrow +} = \int_{I_i}^{\infty} \sqrt{\frac{2E}{m}} Q_{i \rightarrow +}(E; E', E'') f(E) dE \int dE' \int dE''$$

E is the incident energy, E' and E'' the scattered and ejected energies

$$\alpha_{+ \rightarrow i}^{(3)} = 8 \left(\frac{\pi a_0^2 I_H}{kT_{eff}} \right)^{3/2} \frac{\omega_i}{2\omega_+} e^{I_i/kT_{eff}}$$

Three-body recombination

$$\times \int_{I_i}^{\infty} \sqrt{\frac{2E}{m}} Q_{i \rightarrow +}(E; E', E'') f(E) dE$$

Thompson cross-section allows evaluation

$$\times \int \int \left[\frac{\sqrt{\pi}}{2} (kT_{eff})^{3/2} e^{-I_i/kT_{eff}} \right.$$

$$Q_{i \rightarrow +}(E; E', E'') = 4\pi a_0^2 \zeta I_H^2 \frac{1}{EE'^2} \delta(E - E' - E'' - I_i)$$

$$\left. \times \sqrt{\frac{E}{E'E''} \frac{f(E')f(E'')}{f(E)}} \right] dE' dE''$$

5.5 ADAS code schematics

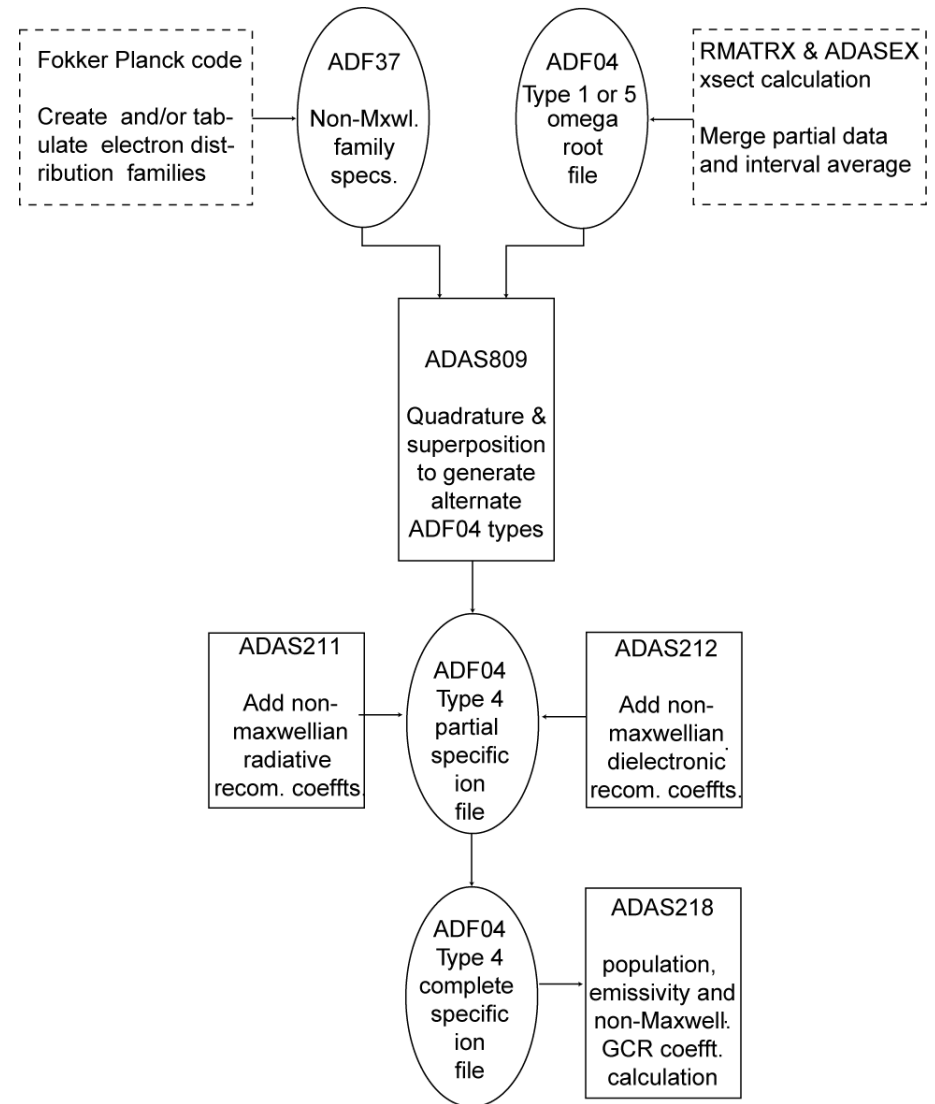
Extension of the adf04 definition allows the non-Maxwellian extension to fit into the existing ADAS framework

Attention to resonant structure in cross-sections is important for realistic rate coefficients. Simple smoothed fits are not valid.

Conversion of raw R-matrix data to usable adf04 type 1 format requires tuned condensation to an acceptable set of energies by interval averaging.

The interval averaging takes account of cross-section energy scale lengths vs distribution function energy scale lengths

Comprehensive studies require valid estimations of electron distribution functions in actual plasma, for example, from a Fokker Planck code.



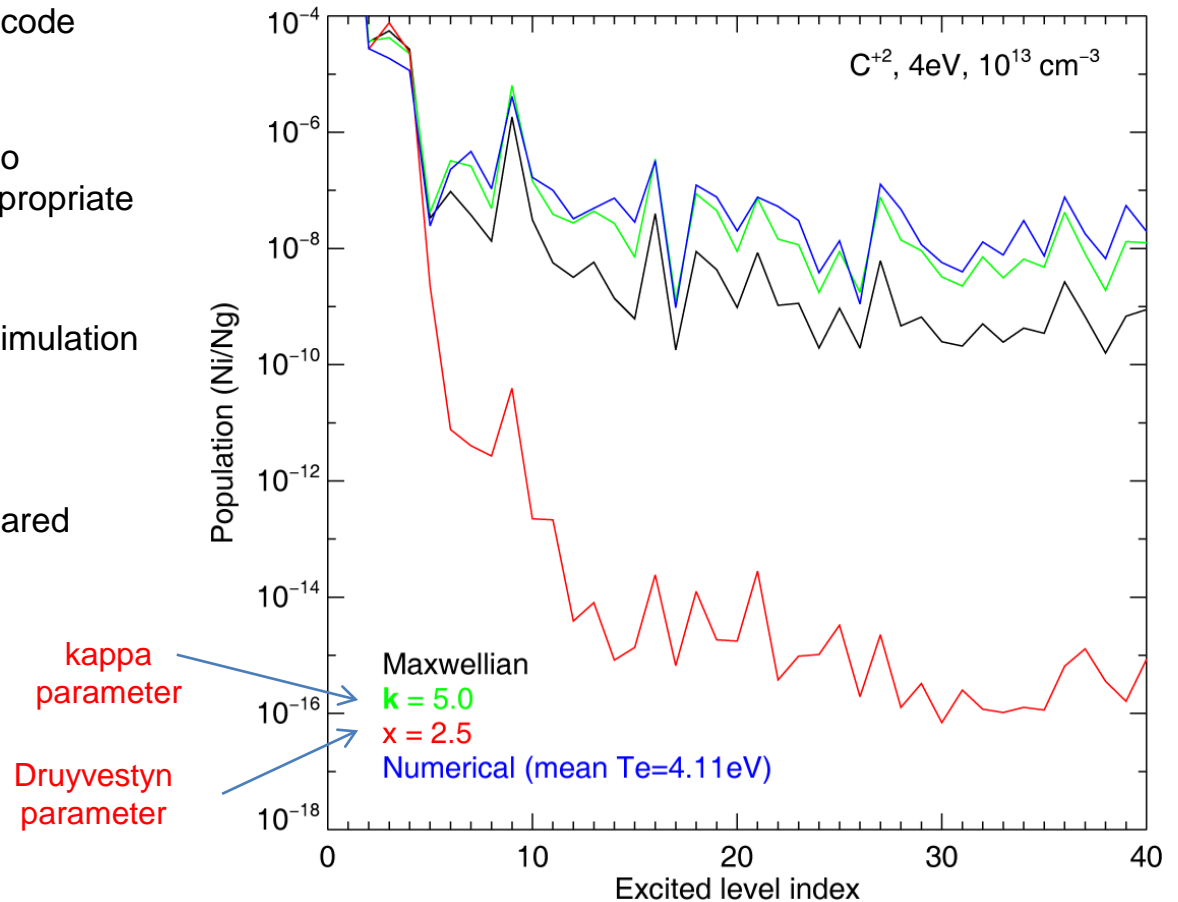
5.6 Non-Maxwellian populations

Non-Maxwellian populations evaluated using code [ADAS218](#).

Differential variation of populations according to enhancement or depletion of regions of the appropriate distribution functions.

The numerical non-Maxwellian is from a JET simulation near the divertor plate by Tskhakaya.

The non-Maxwellian adf04 datasets were prepared for the appropriate distribution functions using [offline_adas/adas7#3/adf04_om2ups](#)



ADAS has wide coverage of type 5 adf04 datasets for non-Maxwellian studies in directory [./adas/adf04/cophps#<ionseq>/dw/<coupling>#<ion>_t5.dat](#).

6.1 Conclusions.

- Spectral analysis of fusion plasma environments has strong similarities with that of the solar upper atmosphere, but with the unique advantages of independent knowledge (from Thompson scattering) of the electron density and temperature profiles across the plasma and multiple lines-of-sight through the plasma.
- The line-of-sight issue has necessitated a technique of analysis in the solar case called differential emission measure analysis (DEM) for inferring the variation of temperature and effective emitting volume with height in the solar atmosphere.
- Attempts to model more complex outer fusion plasma regions of strong gradients, possibly with transient island formation, suggests an extended DEM approach, called 'double-differential emission measure' which can be supported with precisions of atomic data attainable by ADAS GCR modelling.
- Transient events are common to both solar and fusion scenarios and the associated non-linear ionisation state issues are amenable to ADAS modelling and inclusion in a DEM framework.
- Opacity has been of low relevance in fusion (except for hydrogen Lyman lines) but the extended path lengths and low temperatures of divertor scenarios raise this issue for low ionisation stages of light elements, especially carbon. Low to moderate opacity studies, addressed in the escape factor approach has a record of success in solar astrophysics, using ADAS models and data. This is ready for transfer to the fusion case.
- Non-Maxwellian distributions are certainly present in both fusion and astrophysical plasmas and with a need in both to make progress in spectroscopic diagnostic deduction of non-Maxwellian character. ADAS development in this area is comprehensive and is enabling fusion and solar astrophysics to share knowledge and experience.